UNIVERSITY OF LEEDS

White Rose
university consortium
Universities of Leeds, Sheffield & York

eprints@whiterose.ac.uk
https://eprints.whiterose.ac.uk/

Influence of metal addition to Ni-based catalysts for the co-production of carbon nanotubes and hydrogen from the thermal processing of waste polypropylene

Mohamad Anas Nahil[*], Chunfei Wu[*], Paul T. Williams[*]

Energy Research Institute, The University of Leeds, Leeds, LS2 9JT, UK
(Tel: #44 1133432504; Email: p.t.williams@leeds.ac.uk; c.wu@leeds.ac.uk; m.a.nahil@leeds.ac.uk)

ABSTRACT:

This paper investigates the co-production of hydrogen and carbon nanotubes from the pyrolysis-catalytic gasification of waste plastics (polypropylene). We report on the influence of a range of metal additions to a nickel based catalyst based on ternary mixed oxides types Ni-Metal-Al, where the metal was Zn, Mg, Ca, Ce or Mn. The results showed that of the different metal-nickel catalysts investigated, the Ni-Mn-Al catalyst was the most promising catalyst in relation to the co-production of hydrogen and CNT. For example, the Ni-Mn-Al catalyst produced 71.4 mmol hydrogen g^{-1} plastic, while the hydrogen production using Ni-Ca-Al, Ni-Ce-Al and Ni-Zn-Al catalysts were 68.5 mmol g^{-1}, 63.1 mmol g^{-1} and 45.9 mmol hydrogen g^{-1} plastic respectively. In addition, carbon deposition on the catalyst was highest in the order of: Ni-Mn-Al> Ni-Ca-Al> Ni-Zn-Al> Ni-Ce-Al> Ni-Mg-Al. The carbon deposition for the Ni-Mn-Al catalyst was found to consist of mostly carbon nanotubes. Further investigation of the Ni-Mn-Al catalyst demonstrated that the interaction between Ni and catalyst support plays a significant role in the gasification process; weak metal support interaction (for the Ni-Mn-Al catalyst calcined at 300 °C) resulted in a lower hydrogen production and much higher yield of carbon products. In addition, the influence of steam injection rate on hydrogen and carbon nanotube production was investigated for the Ni-Mn-Al catalyst. Increasing the steam injection rate significantly increased hydrogen production and decreased carbon deposition. However, at lower steam injection rates, the quality of the product carbon nanotubes was improved.

KEYWORDS: Waste; Reforming; Gasification; Plastic; Hydrogen; Carbon nanotubes.

1. INTRODUCTION

Hydrogen is expected to become a promising energy carrier for sustainable energy consumption because it possesses high energy density (ca.120.7 kJ/g) and its combustion produces no environmental pollutants [1-3]. Currently, hydrogen is industrially produced by the conversion of fossil fuels, which is considered as unsustainable and in addition, the process also releases greenhouse gases to the environment [4]. There is therefore great interest in producing hydrogen from alternative feedstocks. One such feedstock is waste plastic which can be thermally converted to hydrogen [5]. The world's overall consumption of plastics in 2010 was 230 million tonnes and the predictions are for an upward trend of 3% annual growth in plastics use in developed countries and 10% in developing countries [6]. The rapid rate of plastic consumption throughout the world has led to the creation of increasing amounts of plastic waste. For example, it is estimated that in Europe 25.2 million tonnes of plastic waste is generated each year [7].

The pyrolysis and gasification of waste plastic for hydrogen production have been extensively investigated [6,8-13]. Many catalysts have also been investigated to improve the efficiency of the process and to increase hydrogen production. Ni based catalysts have been reported to be effective for hydrogen production due to their high C–C bond breaking activity with significantly lower cost compared to noble metal catalysts such as Ru, Pt and Rh [14-16]. However, the main problem associated with Ni catalysts is that they suffer from a high deactivation rate caused by the formation of carbonaceous deposits. The deactivation involves covering of the catalyst active sites due to encapsulating by amorphous carbons; in addition carbon filaments and carbon nanotubes are also formed on the surface of the reacted catalyst [14,17,18].

Carbon nanotubes (CNTs) are a unique form of carbon due to their intrinsic properties such as extraordinary mechanical, electric, thermal stability and chemical inertness [19,20].

2

Therefore, production of higher quality CNTs at lower cost is of great importance. Different methods have been developed to produce CNTs including laser ablation [21], arc-discharge [22], chemical vapour deposition [23] and pyrolysis/catalytic steam reforming [24]. Chemical vapour deposition is considered as the most dominant method for CNTs production, while gasification of waste plastics has received less attention. The main advantage of plastic gasification in the presence of steam is that it can produce both CNT and also hydrogen depending on the conditions and the catalyst used. Currently, there are a few reports in relation to the simultaneous production of hydrogen and carbon nanotubes from waste plastics using thermochemical methods [25,26]. In order to increase the quality and quantity of CNTs, more work about catalyst development is needed.

Here, we investigate the influence of metal addition to Ni-based catalysts prepared by co-precipitation to determine their influence on the production of hydrogen and CNT from waste plastics as represented by waste polypropylene. Co-precipitation as a catalyst preparation method has drawn much attention due to its high catalytic effect on hydrogen production. It is well known that the stabilization of Ni catalysts can be enhanced by the incorporation of the active metal into a mixed oxide matrix [27,28]. During the preparation of Ni based catalysts by co-precipitation, different cations can be introduced into the structure and will modify the catalytic properties, such as the particle morphology or metal reducibility in the final catalyst [28-30]. Accordingly, catalytic activity and stability will be directly related to the type of metals incorporated.

In this study, catalytic-steam reforming of waste plastic polypropylene was carried out to investigate the activity of Ni catalysts based on different types of ternary mixed oxides, Ni-Metal-Al, where the added metal was Zn, Mg, Ca, Ce or Mn. The catalysts were prepared by a co-precipitation method and their use in hydrogen and CNT production was investigated

using a two stage fixed bed reactor. Metal addition to the Ni-based catalyst, water injection rate and interaction between Ni metals and catalyst support was studied.

2. Materials and Methods

2.1. Materials

Waste plastic in the form of recovered waste polypropylene (PP) was obtained as 2 mm pellets provided by Regain Polymers Ltd., UK. A series of Ni based catalysts type Ni-Metal-Al (molar ratio 1:1:1) were prepared by a co-precipitation method using the rising pH technique according to the method reported by Garcia et al. [31]. The initial Ni-Metal-Al molar ratio was 1:1:1. As an example, Ni-Zn-Al catalyst was prepared starting with 200 ml of an aqueous solution containing $Ni(NO_3)_2$ $6H_2O$, $Zn(NO_3)_2$ $6H_2O$ and $Al(NO_3)_3$ $9H_2O$. The precipitant, 1M NH_4OH, was added to this solution and the precipitation was carried out at 40 °C with moderate stirring until the final pH of 8.3 was obtained. The precipitates were filtered and washed with water (40 °C), followed by drying at 105 °C overnight, and then they were calcined at 750 °C for 3 h. The other catalysts Ni-Mg-Al, Ni-Ca-Al, Ni-Ce-Al and Ni-Mn-Al were synthesized following the same procedure described above, but replacing Zn nitrates by those of Mg, Ca, Ce and Mn, respectively. All the catalysts used in this paper were crushed and sieved to granules with a size of 65 to 212 µm. In addition, all the catalysts used were not reduced, reduction being carried out by the reducing gases such as hydrogen and carbon monoxide produced during the process.

2.2. Experimental pyrolysis-catalytic steam gasification system

4

Examination of the prepared Ni-Metal-Al catalysts for the purpose of hydrogen and CNT production from catalytic-steam reforming/gasification of waste polypropylene was carried out in a two-stage reaction system (Figure 1). The two-stage fixed bed reaction system consisted of a first stage plastics pyrolysis and a second steam catalytic reforming/gasification stage. Approximately 2 g of waste polypropylene was pyrolysed in the first stage, and the pyrolysis products were passed directly to a second stage where steam catalytic reforming/gasification of the evolved pyrolysis gases was carried out. N_2 gas with a flow rate of 80 ml min^{-1} was used as carrier gas for each experiment and 1 g of the catalyst was used in the second stage.

The experimental procedure consisted of initial heating of the catalyst in the second stage to 800 ºC with a heating rate of 40 °C min^{-1}. Once the second catalyst stage reactor had stabilised at 800 ºC, the waste plastic sample was then pyrolysed at a heating rate of 40 ºC min^{-1} to the final pyrolysis temperature of 500 ºC in the first stage reactor. The evolved pyrolysis volatiles were passed directly to the second stage where water was also introduced and thereby the pyrolysis volatiles were catalytically steam reformed/gasified. The water flow rate used was 4.74 g h^{-1}. Further work involving the Ni-Mn-Al catalyst investigated the influence of different steam flow rates on hydrogen and CNT formation at water injection rates of 0, 2.85, 4.74 and 8.54 g h^{-1}. Two condensers were used to trap the condensable products consisting of an air cooled condenser, followed by a solid CO_2 cooled condenser. The non-condensed gases were collected with a 25 L Tedlar TM gas sample bag. The gases collected in the sample bag were analysed off-line by packed column gas chromatography (GC). Hydrocarbon gases (C_1-C_4) were analysed using a Varian CP-3380 gas chromatograph with a Flame Ionisation Detector (FID) with a 80-100 mesh Hysep column and nitrogen carrier gas. Carbon dioxide, hydrogen, nitrogen, carbon monoxide and oxygen were analysed with a separate Varian CP-3380 gas chromatograph fitted with two separate packed columns

and with two thermal conductivity detectors (GC/TCD). Hydrogen, oxygen and carbon monoxide, methane and nitrogen were analysed on a 2m length by 2mm diameter column, packed with 60-80 mesh molecular sieve. Argon was used as the carrier gas. Carbon dioxide was analysed on a separate 2m length by 2mm diameter column with Haysep 80-100 mesh packing material.

The calibration of the gas chromatograph was carried out prior to the analysis of gas samples obtained from the experiments. Precision standard gas mixtures including alkanes, alkenes and permanent gas mixture were used. In order to calculate the amount of gas in grams, the area obtained for each gas from gas chromatography was compared with the area of calibration gas, and the percentage of each gas in the mixture was calculated. As a known quantity of nitrogen was introduced into the reactor during the experiment and no nitrogen was produced from the experiment, the total gas volume could be calculated using the percentage and the volume of nitrogen. The number of moles for each gas could be then calculated from the volume percentage of each gas and the total gas volume. The number of moles of each gas was converted into grams using its molecular weights, and the total mass of the gas mixture was obtained from the sum of all individual gases.

2.3. Catalyst characterisations

A scanning electron microscope (SEM) (LEO 1530) and a transmission electron microscope (TEM) (FEI Tecnai TF20) were used to study the surface morphology of the reacted catalysts. Raman Spectroscopy (Renishaw Invia) was used to characterise the fresh and reacted catalysts. Temperature programmed oxidation (TPO) was also used to obtain information of coke formation on the reacted catalyst using a thermogravimetric analyser (TGA) (Shimazu). During the TPO analysis, around 20 mg of the reacted catalyst was heated

in an atmosphere of air (50 ml min^{-1}) at a heating rate of 15 °C min^{-1} up to a temperature of 800 °C and with a hold time of 10 minutes. Temperature programmed reduction (TPR) was also used to characterise the fresh catalysts using a Stanton-Redcroft thermogravimetric analyser (TGA). During the TPR analysis, the fresh catalyst was heated at 20 °C min^{-1} to 150 °C and held for 30 min, then heated at 10 °C min^{-1} to 900 °C in an atmosphere of a gas mixture containing 5% H_2 and 95% N_2 (50 ml min^{-1}). The BET (Brunauer, Emmett and Teller) surface area of each catalyst was obtained via nitrogen adsorption experiments using a Quantachrome Corporation Autosorb Instrument

3. Results and Discussion

3.1. Pyrolysis-catalytic steam reforming/gasification of waste polypropylene

3.1.1. Products yield and gas compositions

Different nickel based catalysts were investigated for hydrogen and CNT productions via the pyrolysis-catalytic steam reforming of waste polypropylene using the laboratory scale fixed-bed reaction system. Table 1 shows the influence of metal catalytic activity on the production of gas and hydrogen, as well as percentage of carbon deposited on the catalyst. The water flow rate used was 4.74 g h^{-1}. The results show that the introduction of the steam and catalyst had a positive effect on the gas yield and hydrogen production compared to the absence of a catalyst, where sand was used in place of the catalyst bed. The gas yield was calculated as the amount of gas produced divided by the amount of plastic sample used in the experiment (over 100% gas yield was obtained since the reacted steam was not included). The gas yield was significantly increased in the presence of a catalyst, where the highest gas yield was obtained using the Ni-Mg-Al catalyst (168.4 wt.%). The Ni-Ca-Al and Ni-Ce-Al catalysts showed very similar gas yields (around 148 wt.%). However, the Ni-Mn-Al and Ni-

Zn-Al catalysts produced relatively less gas with about 131.1 wt.% and 120.9 wt.%, respectively.

Regarding the hydrogen production and the carbon deposition, the results showed different trends. Hydrogen production was calculated by the molar amount of produced hydrogen divided by the weight of raw sample. Carbon deposition was calculated as the weight difference of the catalytic bed before and after experiment divided by the feedstock weight. The Ni-Mg-Al catalyst produced the highest hydrogen production (75.4 mmol hydrogen g^{-1} polypropylene) among all the catalysts. The hydrogen production using the Ni-Mn-Al catalyst was 71.4 mmol g^{-1} polypropylene which was more than that produced using the Ni-Ca-Al (68.5 mmol g^{-1}) and Ni-Ce-Al catalysts (63.1 mmol g^{-1}). The lowest hydrogen production was obtained for the Ni-Zn-Al catalyst.

The Ni-Mn-Al catalyst has shown the highest carbon deposition yield (23 wt%), while the Ni-Mg-Al catalyst produced the lowest carbon deposition (3.5 wt%). The carbon deposition yields for the other catalysts were between 3.5 and 23 wt%. The lowest carbon deposition using the Ni-Mg-Al catalyst is consistent with our earlier work [32] where the target product from the process was high hydrogen yield and low catalyst carbon formation for the pyrolysis-gasification of polypropylene.

Table 1 also shows the volumetric concentrations of the product gases (on a nitrogen free basis). From the results, obviously no CO and CO_2 were detected in the gas products in the presence of sand (no catalyst) and without steam. After introduction of steam, CO and CO_2 were generated with concentrations of 1.9 and 1.2 vol%, respectively. However, the introduction of steam in the presence of sand significantly decreased H_2 content from 58.4 to 24.7 vol% with a consequent increase in hydrocarbons gases.

The presence of Ni-Metal-Al catalysts with steam reduces the hydrocarbons gases and increases the hydrogen production as a result of steam reforming reactions. The main gases

produced are H_2 and CO. H_2 concentration is more than 60 Vol.% for the experiment in the presence of the Ni-Mn-Al catalyst, while H_2 concentration produced using other catalysts was in the range of 52.7 to 58.3 Vol.%. The lowest H_2 concentration (52.7 Vol.%) was obtained in the presence of the Ni-Zn-Al catalyst. In addition, some interesting trends related to CO and CO_2 concentrations were also observed. The Ni-Mn-Al catalyst produced relatively lower CO concentration and higher H_2 and CO_2 concentrations compared to the other catalysts. This could be attributed to Ni-Mn-Al catalyst promoting the water gas shift reaction more than the carbon steam gasification, resulting in the highest carbon deposition using the Ni-Mn-Al catalyst.

3.1.2. Characterisation of fresh catalysts

Figure 2 shows the TPR patterns of Ni-Metal-Al catalysts (Metal: Zn, Mg, Ca, Ce and Mn). All the catalysts, except the Ni-Mg-Al catalyst, showed two reduction peaks. The first peak was observed at relatively low temperature between 350-650 °C. This hydrogen consumption could be assigned to the reduction of weakly interacted NiO with the support [33]. The second reduction peak was detected in all catalysts used at temperatures over 700°C. This peak was attributed to the Ni^{2+} reduction with a high degree of interaction with the modified support.

According to the amount of hydrogen and carbon deposition yields presented in Table 1, the TPR results (Figure 2) have a clear relation to the hydrogen and carbon production from pyrolysis-catalytic steam reforming of polypropylene. For example, the Ni-Mn-Al catalyst shows the highest intensity of H_2 reduction at around 400 °C during the TPR analysis indicating weak metal support interaction [34]. This is suggested to result in the highest carbon deposition on the reacted Ni-Mn-Al catalyst (Table 1). The strongest metal support interaction was obtained for the Ni-Mg-Al catalyst (Figure 2) suggesting the lowest carbon

formation. The results are consistent with the literature [35,36]. To investigate more the relation between the metal support interaction for the Ni-Mn-Al catalyst and the carbon deposition, a Ni-Mn-Al catalyst with weaker metal support interaction was prepared. This was performed by calcination of the catalyst at lower temperature (300°C) for 3 hours. Figure 2 also shows the TPR patterns of Ni-Mn-Al catalyst prepared at calcination temperatures of 300 °C. Two reduction peaks were observed in this catalyst. As discussed above, the first peak observed at relatively low temperature could be assigned to the reduction of NiO which was weakly interacted with the support. While the reduction peak detected at higher temperature is attributed to the Ni^{2+} reduction with a high degree of interaction with the support. The Ni-Mn-Al catalyst prepared at a calcination temperature of 300 °C has a stronger reduction peak at lower temperature and weaker reduction peak at higher temperature compared to the Ni-Mn-Al catalyst prepared at the calcination temperature of 750 °C. Pyrolysis-catalytic steam reforming of waste polypropylene using these two catalysts with a water flow rate of 4.74 g h^{-1} was performed. The results showed that the hydrogen production decreased from 71.4 to 52.4 mmol hydrogen g^{-1} plastic and the carbon deposition yield increased from 23 to 57 wt% when the calcination temperature of the Ni-Mn-Al catalyst was changed from 750 to 300 °C. This confirms that the first reduction peak was responsible for the carbon deposition while the hydrogen production can be linked directly to the second reduction peak.

3.2. Carbon nanotubes production

3.2.1. SEM analysis

Figure 3 shows scanning electron micrographs (SEM) of the different reacted metal-Ni based catalysts. SEM observations show that carbons in the form of filamentous carbons were clearly produced upon the Ni-Mn-Al catalyst. Long, smooth and thin filamentous carbons can

be observed on the reacted Ni-Mn-Al catalyst with average diameter of about 20 nm. However, filamentous carbons were difficult to be observed on the surface of the other catalysts. This could be directly related to the type of metal in the catalyst. We show later that the filamentous carbons are largely carbon nanotubes (Sections 3.3.2. and 3.3.3.). It has been reported that, the composition of the catalyst is considered as one of the main factors that affects the production of carbon nanotubes [37,38]. Latorre et al. [39] investigated the effect of catalyst composition on hydrogen and carbon nanotubes production. They found that the catalyst activity, selectivity and resistance to deactivation during the production of hydrogen and carbon nanotubes by catalytic decomposition of methane depend directly on the catalyst composition. The ranges of reaction temperatures where the catalysts are active and stable are mainly determined by the catalyst composition.

3.2.2. TPO analysis

Temperature-programmed oxidation (TPO) analysis was carried to investigate the nature and the amount of carbons deposited on the catalyst surface. Figure 4 shows the TPO results of all the reacted catalysts. For example, during the TPO analysis, the mass of reacted catalyst firstly reduced, then increased and finally decreased to a stable level except for the Ni-Zn-Al catalyst which showed almost no weight reduction. The mass loss observed at a temperature up to 100 ℃ is due to water vaporization which could be absorbed by the reacted catalysts. The mass increase in the TPO results are due to the oxidation of metallic Ni. It is well known that the Ni phase is produced from the reduction of NiO by reducing agents such as CO and H_2 during the pyrolysis-gasification process [40,41]. The final decrease of the mass is due to the oxidation of deposited carbon on the catalyst. The results show that the oxidation of carbon started after 400 ℃ for the Ni-Ce-Al and Ni-Mg-Al catalysts and after 580 ℃ for the Ni-Ca-Al and Ni-Mn-Al catalysts. The continuous increase in the weight of the

Ni-Zn-Al catalyst suggests that this catalyst contains a high content of Ni phase and the lowest coke deposition.

In order to distinguish between amorphous and filamentous carbons, for Figure 4, the weight loss between 400 and 600 °C was attributed to the oxidation of amorphous carbons and the weight loss after 600 °C is attributed to the oxidation of filamentous carbons, during the TPO analysis [10,12,13]. Therefore, the Ni-Ca-Al and Ni-Mn-Al catalysts produced larger quantity of filamentous carbons compared to the other catalysts. This could be due to the metal particle size and the support structure.

Sakae et al. [42] investigated the decomposition of methane into carbon and hydrogen over Ni catalysts on different supports, including SiO_2, TiO_2, graphite, Al_2O_3, MgO and $SiO_2 \cdot MgO$. According to their results, Ni particle size determines the quantity of hydrogen and the diameter of CNTs while the support porosity structure will determine the quantity of CNTs and their length. They found also that the quantity and the length of CNTs increased as the porosity decreased. They proposed that if the tip of a carbon filament came in contact with the wall of other carbon filaments or with the inside walls of the supports during the methane decomposition, the growth of the carbon should unavoidably be stopped [42]. In this study, it was found that the Ni-Mn-Al catalyst had the poorest porosity structure with the lowest BET surface area of 20 m^2 g^{-1} compared to the porosity of other catalysts. Ni-Ca-Al, Ni-Zn-Al, Ni-Mg-Al and Ni-Ce-Al catalysts had BET surface areas of 28, 53, 55 and 66 m^2 g^{-1} respectively. This might explain why the Ni-Ca-Al and Ni-Mn-Al catalysts produced a larger quantity of filamentous carbons compared to the other catalysts. In addition, a three-step VSS (vapor-solid-solid) mechanism has been reported for the growth of carbon nanotubes; including the dissociation of carbon precursor, carbon diffusion on the surface of catalyst and carbon precipitation [43]. In most of the cases, metal particles e.g. Ni are lifted during the growth of CNTs [44]. The weak interaction between Ni and the catalyst support

12

would increase the availability of free Ni particles involved in CNTs production [45]; therefore, Ni-Mn-Al catalyst calcined under lower temperature having weak metal-support interaction (Figure 2) produced more CNTs compared with the Ni-Mn-Al calcined at 750 °C.

From the above results, the Ni-Mn-Al catalyst generated the highest amount of filamentous carbons and also a reasonable yield of hydrogen. Therefore the Ni-Mn-Al catalyst was regarded as a promising catalyst for the simultaneous production of both CNT and hydrogen, and was selected for further study with various steam feeding rates to the reaction system.

3.3. CNT and hydrogen production with the Ni-Mn-Al catalyst

3.3.1. Products yields and gas compositions

The influence of steam addition in the presence of the Ni-Mn-Al catalyst was investigated in relation to the production of hydrogen and carbon deposition using water injection rates of 0, 2.85, 4.74 and 8.54 g h^{-1}. The gas yield and hydrogen production corresponding to the different water flow rates is presented in Table 2. From Table 2, the gas yield and the hydrogen production significantly increased from 23.8 wt.% to 193.6 wt.% and 50.7 mmol hydrogen g^{-1} plastic to 90.1mmol hydrogen g^{-1} plastic respectively, when the water injection rate was increased from 0 to 8.54 g h^{-1}. However, the carbon deposition decreased from 62 wt.% to 10 wt.% with increasing water injection rate from 0 to 8.54 g h^{-1}. The gas composition results in relation to injected water flow rate are also shown in Table 2. The H_2 concentration decreased from 86.4 to 61.0 vol .%, CO_2 increased from 0 to 3.7 vol.%, CO increased from 0 to 22.5 vol.%, and CH_4 decreased, when the water flow rate was increased from 0 to 2.85 g h^{-1}.

A small influence on gas composition was observed as the water injection flow rate was increased from 2.85 to 8.54 g h^{-1}. The H_2 concentration slightly increased, CO decreased

and CO_2 increased when the water injection rate was increased from 2.85 to 4.74 g h^{-1}. This is mainly due to the hydrocarbon reforming reaction and the water gas shift reaction. Further increase in the water injection flow rate to 8.54 g h^{-1} leads to an increase in CO and CO_2 with almost no effect on H_2 and hydrocarbon gases. This could be attributed to the gasification of deposited carbon which can be confirmed by the considerable decrease in the carbon deposition (Table 2) [46].

3.3.2. SEM and TEM analysis of reacted Ni-Mn-Al catalyst

Figure 5 shows the SEM micrographs of the reacted Ni-Mn-Al catalysts. For the water injection rates of 0, 2.85 and 4.74 g h^{-1} the carbon deposition was mainly highly entangled filamentous carbons. The diameter of carbon filaments decreased as the steam injection flow rate was increased from 0 to 4.74 g h^{-1}. In addition, the length of the carbon filaments was increased, when the steam injection flow rate was increased to 4.74 g h^{-1}. With the further increase of steam injection rate to 8.54 g h^{-1}, the steam reacted with the carbon deposits to produce more hydrogen but at the same time removed the carbon from the catalyst (Table 2). The SEM micrograph of the used catalyst at water injection rate of 8.54 g h^{-1}, showed only low levels of filamentous carbons. It is suggested that most of the carbons deposited on the surface of the catalyst are amorphous carbons at water injection rate of 8.54 g h^{-1}.TEM images of the reacted Ni-Mn-Al catalyst with a water injection rate of 4.74 g h^{-1} are shown in Figure 6, confirming that most of the carbon deposition was bamboo-like carbon nanotubes and that the CNTs produced were multi-walled carbon nanotubes (MCNTs) with parallel graphene layers.

From the SEM micrographs and the carbon deposition results, it can be concluded that the quantity of steam plays an important role in the morphology, the quality and the quantity of carbon nanotubes produced. Tobias et al. [47] reported that steam can be used effectively

for purification of CNTs since steam is a mild oxidizing agent which can remove the amorphous carbon present in samples with less defects on the produced CNTs. Therefore, the results suggest that using Ni-Mn-Al catalyst with steam injection rate of 4.74 g h^{-1} is optimal for both hydrogen and CNT production in this work.

3.3.3. Raman analysis for reacted Ni-Mn-Al catalyst

The carbon deposits on the used Mn-Ni-Al catalysts were studied by laser Raman spectroscopy, to determine the crystalline and amorphous carbon present (Figure 7). The carbon species show spectral bands in the range of 1000-1700 cm^{-1} and more specifically at approximately 1560 cm^{-1} (G band) and 1360 cm^{-1} (D band) where the excitation is in the visible region. In addition, the G' band was observed at ~2690 cm^{-1}. The G-band is attributed to the stretching mode of carbon sp2 bonds of ordered graphite, while the D-band is ascribed to the vibrations of carbon atoms with dangling bonds in disordered amorphous carbon [48]. The G' band is a second order two-phonon process, which indicates the purity of CNTs [49]. Bands D, G and G' are deconvoluted to determine their areas and to evaluate the I_D/I_G and $I_{G'}/I_G$ ratio. Quantifying disorder in a graphene is usually made by analysing the intensity ratio (I_D/I_G) between the disorder-induced D-band and ordered graphite G band, while the intensity ratio ($I_{G'}/I_G$) is used to evaluate the degree of crystallinity of CNTs.

According to the Raman spectroscopy analysis results (Figure 7), interesting differences in the relative intensity of the bands can be observed. For the Ni-Mn-Al catalyst used without steam injection, the D-band is more intense than the G-band (I_D/I_G=1.22) indicating a predominance of disordered carbon, such as amorphous or defective filamentous. Significant changes were observed by the addition of steam. For example, the I_D/I_G ratio decreased to 0.89 using a steam injection rate of 2.85 g h^{-1} and to 0.85 using a steam injection rate of 4.74 g h^{-1}. In contrast, the $I_{G'}/I_G$ ratio increased from 0.55 to 1.39 as the steam injection

rate was increased from 0 to 4.74 g h^{-1}. Therefore, the quality of the carbon nanotubes in terms of purity was improved when the steam was added with the injection rate of 2.85 or 4.74 g h^{-1}. It is suggested that amorphous carbons were removed in the presence of a certain amount of steam [47]. The carbon deposits on the surface of Ni-Mn-Al catalyst with weaker metal support interaction, prepared by the calcination at lower temperature (300°C), were also characterized using laser Raman spectroscopy. The results showed that the I_D/I_G and the $I_{G'}/I_G$ ratios were almost the same using both catalyst samples calcined at 300 and 750°C. According to the these observations, it can be concluded that the nature of the interaction between the Ni particles and the support will affect the hydrogen production and carbon deposition yield but has little influence on the distribution of crystalline and amorphous carbon. However, Raman spectral bands were difficult to be observed using the steam injection rate of 8.54 g h^{-1} demonstrating that most of the deposited carbon was gasified at high steam injection rate. This result is consistent with the SEM analysis (Figure 5), where CNTs could be barely observed on the surface of the reacted Ni-Mn-Al catalyst with the steam injection rate of 8.54 g h^{-1}.

4. Conclusions

   Multi-walled carbon nanotubes have been produced and investigated as a by-product of hydrogen formation from the pyrolysis-catalytic reforming/gasification of waste polypropylene, in the presence of various Ni-based catalysts. The influence of different water injection rates on one of the catalysts (Ni-Mn-Al) was also investigated. The following conclusions were obtained;

1. The Ni-Mn-Al catalyst could be considered as an optimal catalyst among the Ni-based catalysts investigated in relation to hydrogen and carbon nanotube production. The Ni-Mn-Al catalyst generated the highest amount of filamentous carbons and a

reasonably high yield of hydrogen. TEM and Raman spectroscopy analysis of the filamentous carbons confirmed that they were mostly carbon nanotubes.

2. The presence of Ni metal particles on the support and the interaction between Ni and the support were found to be essential for the production of filamentous carbons. The nature of this interaction between the Ni particles and the support will affect the hydrogen production and carbon deposition but will not affect the distribution of crystalline and amorphous carbon. The weaker interaction between the metal and catalyst support results in higher carbon deposition and lower hydrogen production.

3. For the Ni-Mn-Al catalyst, the amount of steam addition significantly increased the hydrogen production but also decreased the amount of carbon deposition. The quality of CNTs in terms of purity and morphology appears to be improved (SEM and Raman analysis) with the increase of water injection rate from 0 to 4.74 g h^{-1}. However, CNTs could barely be observed when the water injection rate to the reaction system was high (8.54 g h^{-1}) indicating the importance of steam in the reaction system for the growth of carbon nanotubes, and also the majority of carbons derived from 8.54 g h^{-1} water injection rate are amorphous carbons.

REFERENCES

[1] S.J. Han, Y. Bang, J. Yoo, J. J.G. Seo, I.K. Song. Hydrogen production by steam reforming of ethanol over mesoporous Ni–Al2O3–ZrO2 xerogel catalysts: Effect of nickel content. International Journal of Hydrogen Energy 38 (2013), 8285-8292.

[2] M.H. Youn, J.G. Seo, H. Lee, Y. Bang, J.S. Chung, I.K. Song. Hydrogen production by auto-thermal reforming of ethanol over nickel catalysts supported on metal oxides: Effect of support acidity Applied Catalysis B: Environmental 98 (2010), 57-64.

[3] A. Haryanto, S. Fernando, N. Murali, S. Adhikari, Current Status of Hydrogen Production Techniques by Steam Reforming of Ethanol: A Review. Energy & Fuels 19 (2005), 2098-2106.

[4] J. Wang, G. Cheng, G. Y. You, B. Xiao, S. Liu, P. He, D. Guo, X. Guo, G. Zhang. Hydrogen-rich gas production by steam gasification of municipal solid waste (MSW) using NiO supported on modified dolomite. International Journal of Hydrogen Energy 37 (2012), 6503-6510.

[5] A. Adrados, I. de Marco, B.M. Caballero, A. López, M.F. Laresgoiti, A. Torres. Pyrolysis of plastic packaging waste: A comparison of plastic residuals from material recovery facilities with simulated plastic waste. Waste Management 32 (2012), 826-832.

[6] A. Erkiaga, G. Lopez, M. Amutio, J. Bilbao, M. Olazar. Syngas from steam gasification of polyethylene in a conical spouted bed reactor. Fuel 109 (2013), 461-469.

[7] Plastics Europe; Association of Plastics Manufacturers Europe, Plastics the Facts -2013. Plastics Europe, Brussels, 2013.

[8] P. Kaewpengkrow, D. Atong, V. Sricharoenchaikul. Pyrolysis and gasification of landfilled plastic wastes with Ni-Mg-La/Al2O3 catalyst. Environmental Technology 33 (2012), 2489-2495.

[9] V. Wilk, H. Hofbauer. Conversion of mixed plastic wastes in a dual fluidized bed steam gasifier. Fuel 107 (2013), 787-799.

[10] J.C. Acomb, M.A. Nahil, P.T. Williams, P.T. Thermal processing of plastics from waste electrical and electronic equipment for hydrogen production. Journal of Analytical & Applied Pyrolysis 103 (2013), 320-327.

[11] J.W. Lee, T.U. Yu, J.W. Lee, J.H. Moon, H.J. Jeong, S.S. Park, W. Yang, U.D. Lee. Gasification of Mixed Plastic Wastes in a Moving-Grate Gasifier and Application of the Producer Gas to a Power Generation Engine. Energy & Fuels 27 (2013), 2092-2098.

[12] C. Wu, P.T. Williams. Pyrolysis–gasification of plastics, mixed plastics and real-world plastic waste with and without Ni–Mg–Al catalyst Fuel 89 (2010), 3022-3032.

[13] C. Wu, P.T. Williams. Pyrolysis–gasification of post-consumer municipal solid plastic waste for hydrogen production International Journal of Hydrogen Energy 35 (2010), 949-957.

[14] M.N. Barroso, A.E. Galetti, M.F. Gomez, L.A. Arrúa, M.C. Abello. Ni-catalysts supported on ZnxMg1-xAl2O4 for ethanol steam reforming: Influence of the substitution for Mg on catalytic activity and stability. Chemical Engineering Journal 222 (2013), 142-149.

[15] M.C. Sánchez-Sánchez, R.M. Navarro, J.L.G. Fierro. Ethanol steam reforming over (La, Zr and Mg) catalysts: Influence of support on the hydrogen production. International Journal of Hydrogen Energy 32 (2007), 1462-1471.

[16] L.F. Bobadilla, S. Palma, S. Ivanova, M.I. Domínguez, F. Romero-Sarria, M.A. Centeno, J.A. Odriozola. Steam reforming of methanol over supported Ni and Ni–Sn nanoparticles. International Journal of Hydrogen Energy 38 (2013), 6646-6656.

[17] L.V. Mattos, G. Jacobs, B.H. Davis, F.B. Noronha. Production of Hydrogen from Ethanol: Review of Reaction Mechanism and Catalyst Deactivation. Chemistry Reviews 112 (2012), 4094-4123.

[18] S. Ahmed, A. Aitani, F. Rahman, A. Al-Dawood, F. Al-Muhaish. Decomposition of hydrocarbons to hydrogen and carbon. Applied Catalysis A: General 359 (2009), 1-24.

[19] G. Wang, H. Wang, Z. Tang, W. Li, J. Bai. Simultaneous production of hydrogen and multi-walled carbon nanotubes by ethanol decomposition over Ni/Al2O3 catalysts. Applied Catalysis B: Environmental 88 (2009), 142-151.

[20] P.K. Seelam, M. Huuhtanen, A. Sápi, M. Szabó, K. Kordás, E. Turpeinen, G. Tóth, R.L. Keiski. CNT-based catalysts for H2 production by ethanol reforming. International Journal of Hydrogen Energy 35 (2010), 12588-12595.

[21] C.D. Scott, S. Arepalli, P. Nikolaev, R.E. Smalley. Growth mechanisms for single-wall carbon nanotubes in a laser-ablation process. Applied Physics A 72 (2001), 573-580.

[22] H.W. Zhu, X.S. Li, B. Jiang, C.L. Xu, Y.F. Zhu, D.H. Wu, X.H. Chen. Formation of carbon nanotubes in water by the electric-arc technique. Chemical Physics Letters 366 (2002), 664-669.

[23] A.A. Koós, M. Dowling, K. Jurkschat, A. Crossley, N. Grobert. Effect of the experimental parameters on the structure of nitrogen-doped carbon nanotubes produced by aerosol chemical vapour deposition. Carbon 47 (2009), 30-37.

[24] C. Wu, J. Huang, P.T. Williams. Carbon nanotubes and hydrogen production from the reforming of toluene. International Journal of Hydrogen Energy 38 (2013), 8790-8797.

[25] J. Gong, J. Liu, L. Ma, X. Wen, X. Chen, D. Wan, H. Yu, Z. Jiang, E. Borowiak-Palen, T. Tang. Effect of Cl/Ni molar ratio on the catalytic conversion of polypropylene into Cu–Ni/C composites and their application in catalyzing "Click" reaction. Applied Catalysis B: Environmental 117 (2012), 185-193.

[26] M.A. Nahil, X. Wang, C. Wu, H. Yang, H. Chen, P.T. Williams. Novel bi-functional Ni-Mg-Al-CaO catalyst for catalytic gasification of biomass for hydrogen production with in situ CO2 adsorption. RSC Advances 3 (2013), 5583-5590.

[27] R. Guil-López, R.M. Navarro, M.A. Peña, J.L.G. Fierro. Hydrogen production by oxidative ethanol reforming on Co, Ni and Cu ex-hydrotalcite catalysts. International Journal of Hydrogen Energy 36 (2011), 1512-1523.

[28] A.J. Vizcaíno, M. Lindo, A. Carrero, J.A. Calles. Hydrogen production by steam reforming of ethanol using Ni catalysts based on ternary mixed oxides prepared by coprecipitation. Internatioanl Journal of Hydrogen Energy 37 (2012), 1985-1992.

[29] S. Velu, K. Suzuki, M. Vijayaraj, S. Barman, C.S. Gopinath. In situ XPS investigations of Cu1−xNixZnAl-mixed metal oxide catalysts used in the oxidative steam reforming of bio-ethanol. Applied Catalysis B: Environmental 55 (2005), 287-299.

[30] A.F. Lucrédio, J.D.A. Bellido, E.M. Assaf. Effects of adding La and Ce to hydrotalcite-type Ni/Mg/Al catalyst precursors on ethanol steam reforming reactions. Applied Catalysis A: General 388 (2010), 77-85.

[31] L. Garcia, A. Benedicto, E. Romeo, M.L. Salvador, J. Arauzo, R. Bilbao. Hydrogen Production by Steam Gasification of Biomass Using Ni−Al Coprecipitated Catalysts Promoted with Magnesium. Energy & Fuels 16 (2002), 1222-1230.

[32] C. Wu, P.T. Williams. Hydrogen production by steam gasification of polypropylene with various nickel catalysts. Applied Catalysis B: Environmental 87 (2009), 152-161.

[33] A.E. Galetti, M.F. Gomez, L.A. Arrúa, M.C. Abello. Ni catalysts supported on modified ZnAl2O4 for ethanol steam reforming. Applied Catalysis A: General 380 (2010), 40-47.

[34] I. Rossetti, A. Gallo, V. Dal Santo, C.L. Bianchi, V. Nichele, M. Signoretto, E. Finocchio, G. Ramis, A. Di Michele. Nickel Catalysts Supported Over TiO2, SiO2 and ZrO2 for the Steam Reforming of Glycerol. ChemCatChem 5 (2013), 294-306.

[35] C. Wu, Z. Wang, L. Wang, J. Huang, P.T. Williams. Catalytic Steam Gasification of Biomass for a Sustainable Hydrogen Future: Influence of Catalyst Composition. Waste & Biomass Valorization 5 (2013), 175-180.

[36] S.S. Maluf, E.M. Assaf. Ni catalysts with Mo promoter for methane steam reforming Fuel 88 (2009), 1547-1553.

[37] Y.H. Chung, S. Jou. Carbon nanotubes from catalytic pyrolysis of polypropylene. Materials Chemistry & Physics 92 (2005), 256-259.

[38] Z. Yang, Q. Zhang, G. Luo, J.Q. Huang, M.Q. Zhao, F. Wei. Coupled process of plastics pyrolysis and chemical vapor deposition for controllable synthesis of vertically aligned carbon nanotube Applied Physics A 100 (2010), 533-540.

[39] N. Latorre, F. Cazaña, V. Martínez-Hansen, C. Royo, E. Romeo, A. Monzón. Ni-Co-Mg-Al catalysts for hydrogen and carbonaceous nanomaterials production by CCVD of methane. Catalysis Today 172 (2011), 143-151.

[40] C. Wu, L. Wang, P.T. Williams, J. Shi, J. Huang. Hydrogen production from biomass gasification with Ni/MCM-41 catalysts: Influence of Ni content. Applied Catalysis B: Environmental 108 (2011), 6-13.

[41] C. Wu, Z. Wang, V. Dupont, J. Huang, P.T. Williams. Nickel-catalysed pyrolysis/gasification of biomass components. Journal of Analytical & Applied Pyrolysis 99 (2013), 143-148.

[42] S. Takenaka, H. Ogihara, I. Yamanaka, K. Otsuka. Decomposition of methane over supported-Ni catalysts: effects of the supports on the catalytic lifetime. Applied Catalysis A: General 217 (2001), 101-110.

[43] J-P. Tessonnier, D. Sheng Su. Recent Progress on the Growth Mechanism of Carbon Nanotubes: A Review. ChemSusChem 4 (2011), 824-847.

[44] Z. Liu, L. Jiao, Y. Yao, X. Xian, J. Zhang. Aligned, Ultralong Single-Walled Carbon Nanotubes: From Synthesis, Sorting, to Electronic Devices. Advanced Materials 22 (2010), 2285-2310.

[45] W. Zhou, Z. Han, J. Wang, Y. Zhang, Z. Jin, X. Sun, Y. Zhang, C. Yan, Y. Li. Copper Catalyzing Growth of Single-Walled Carbon Nanotubes on Substrates. Nano Letters 6 (2006), 2987-2990.

[46] J.C. Acomb, C. Wu, P.T. Williams. Control of steam input to the pyrolysis-gasification of waste plastics for improved production of hydrogen or carbon nanotubes. Applied Catalysis B: Environmental 147 (2013), 571-584.

[47] G. Tobias, L. Shao, C.G. Salzmann, Y. Huh, M.L.H. Green. Purification and Opening of Carbon Nanotubes Using Steam. Journal of Physical Chemistry B 110 (2006), 22318-22322.

[48] A. Carrero, J.A. Calles, A.J. Vizcaíno. Effect of Mg and Ca addition on coke deposition over Cu–Ni/SiO2 catalysts for ethanol steam reforming. Chemical Engineering Journal 163 (2010), 395-402.

[49] M.S. Dresselhaus, A. Jorio, M. Hofmann, G. Dresselhaus, R. Saito, R. Perspectives on Carbon Nanotubes and Graphene Raman Spectroscopy. Nano Letters 10 (2010), 751-758.

Table 1. Production of gas, hydrogen and carbons from pyrolysis-gasification of polypropylene (PP) with different Nickel based catalysts

Catalyst	Sand	Sand and steam	Ni-Zn-Al	Ni-Mg-Al	Ni-Ca-Al	Ni-Ce-Al	Ni-Mn-Al
Gas yield (wt.%)	47.2	74.3	120.9	168.4	148.2	148.6	131.1
Carbon deposition (wt%)	42	7	10	3.5	9.5	8	23
Hydrogen (mmol g^{-1} PP)	26.9	9.4	45.9	75.4	68.5	63.1	71.4
Gas concentrations (vol.%)							
CO	0.0	1.9	19.5	26.9	23.7	24.9	20.9
H_2	58.4	24.7	52.7	56.9	58.3	55.6	62.7
CO_2	0.0	1.2	5.0	3.5	4.4	3.9	5.4
CH_4	26.9	33.2	13.4	9.8	9.4	10.6	9.2
C_2-C_4	14.7	38.9	9.4	2.8	4.3	5.0	1.8

Table 2. Production of gas, hydrogen and carbons from pyrolysis-gasification at different water flow rate with Ni-Mn-Al catalyst

Catalyst	Ni-Mn-Al No steam	Ni-Mn-Al 2.85	Ni-Mn-Al 4.74	Ni-Mn-Al 8.54
Gas yield (wt.%)	23.8	104.8	131.1	193.6
Carbon deposition (wt%)	62	24.5	23	10
Hydrogen (mmol g^{-1} PP)	50.7	54.2	71.4	90.1
Gas concentrations (vol.%)				
CO	0.0	22.5	20.9	23.5
H_2	86.4	61.0	62.7	59.4
CO_2	0.0	3.7	5.4	7.3
CH_4	12.6	8.9	9.2	8.6
C_2-C_4	0.9	3.9	1.8	1.3

Figure Captions

Fig. 1. Schematic diagram of the pyrolysis-reforming of waste plastic

Fig. 2. TPR analysis of different fresh catalysts; Ni-catalyst with different metal additions calcined at 750 °C and Ni-Mn-Al catalyst calcined at 300 °C.
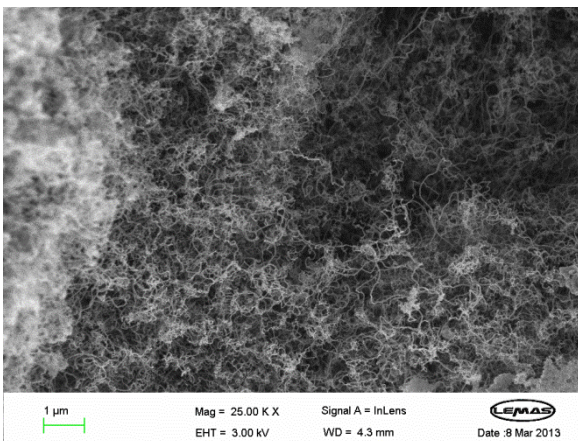
Fig. 3. Scanning electron micrographs of different reacted catalysts.

Fig. 4. Temperature program oxidation (TPO) analysis of different reacted catalysts in the presence of steam injection.

Fig. 5. Scanning electron micrographs of the reacted Ni-Mn-Al catalyst in the presence of different steam injections.

Fig. 6. TEM analysis of the reacted Ni-Mn-Al catalyst with steam injection of 4.74 g h^{-1}

Fig. 7. Raman spectroscopy of the reacted Ni-Mn-Al catalyst; Ni-Mn-Al reacted at different steam injection rates calcined at 750 °C and Ni-Mn-Al catalyst calcined at 300 °C
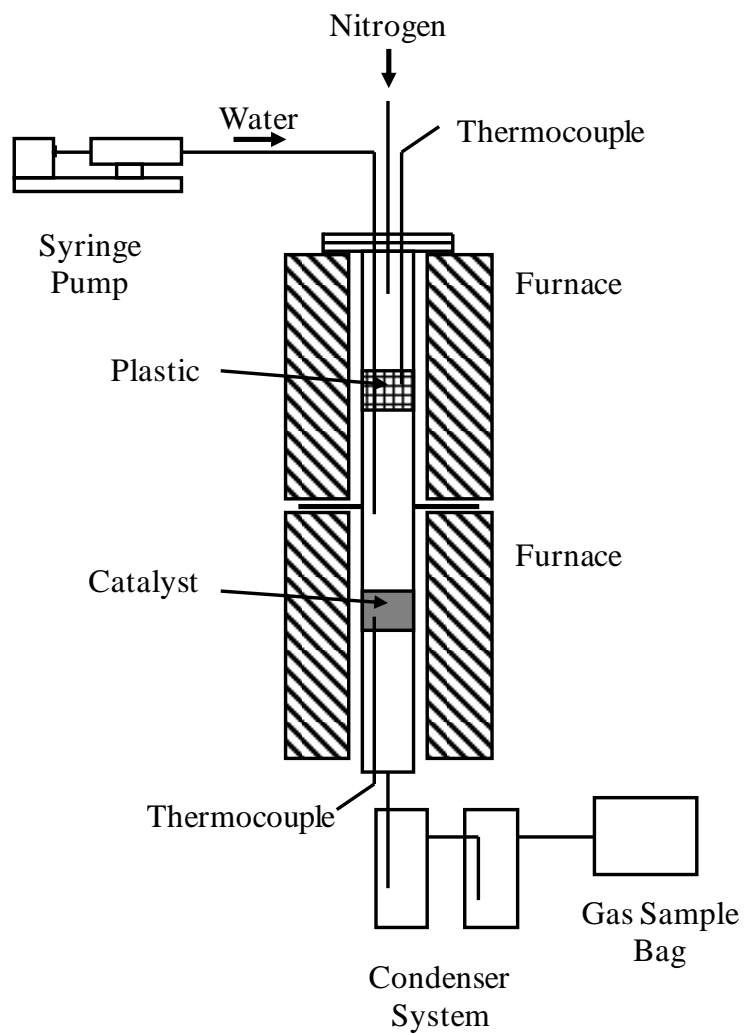
Fig. 1. Schematic diagram of the pyrolysis-reforming of waste plastic
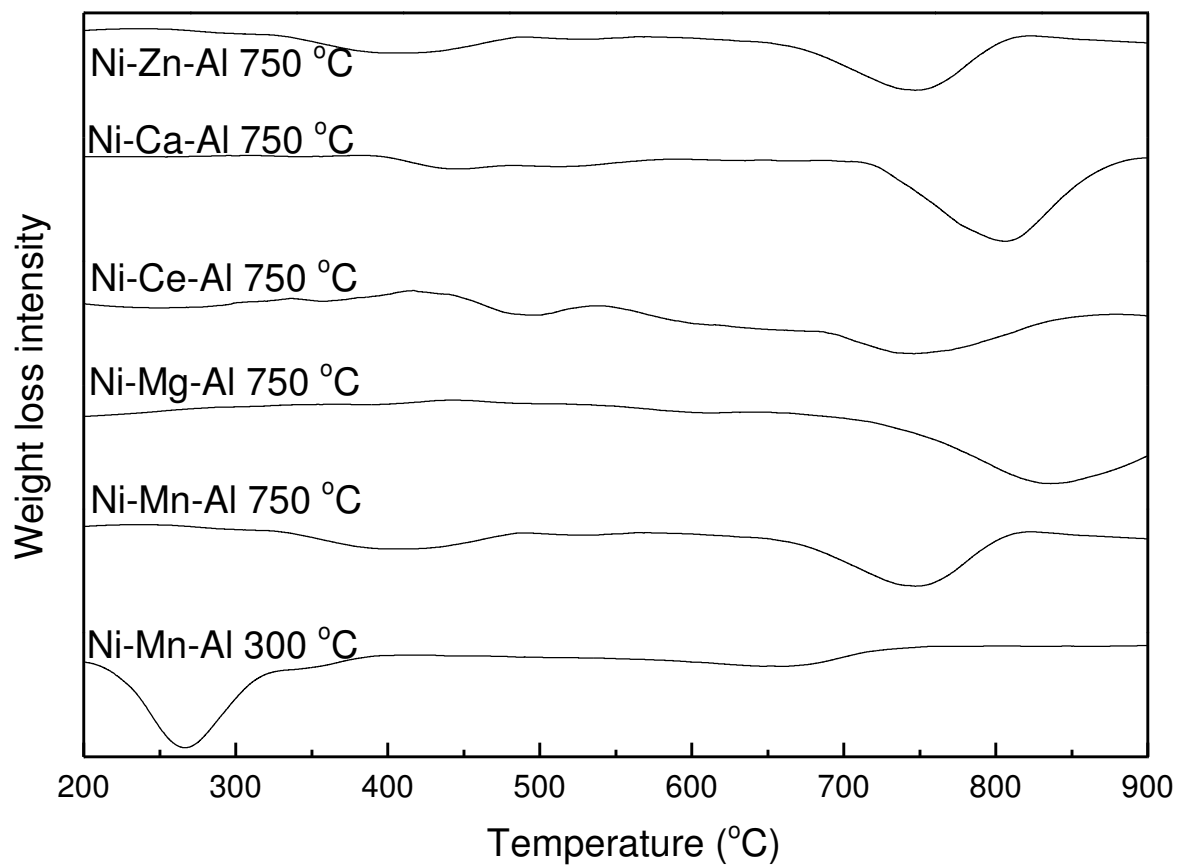
Fig. 2. TPR analysis of different fresh catalysts; Ni-catalyst with different metal additions calcined at 750 °C and Ni-Mn-Al catalyst calcined at 300 °C
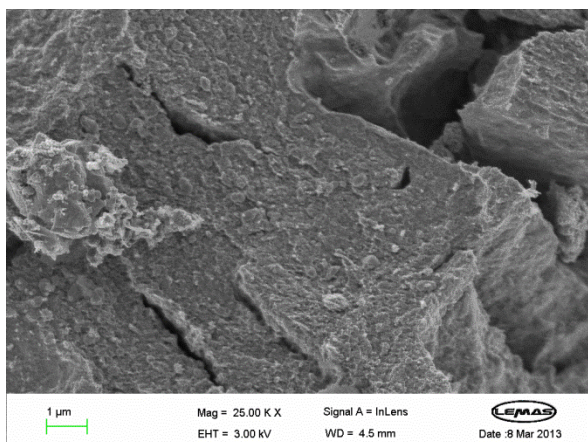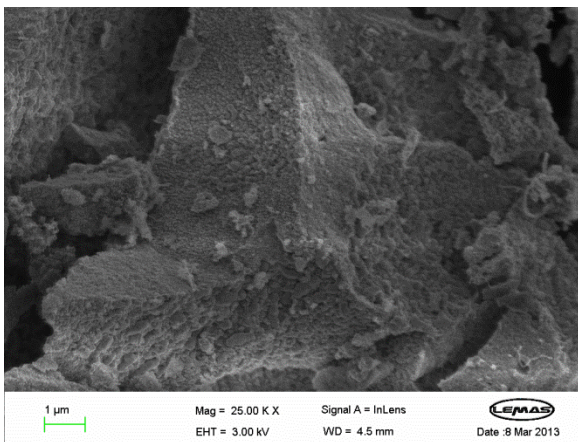
Ni-Zn-Al   Ni-Mg-Al
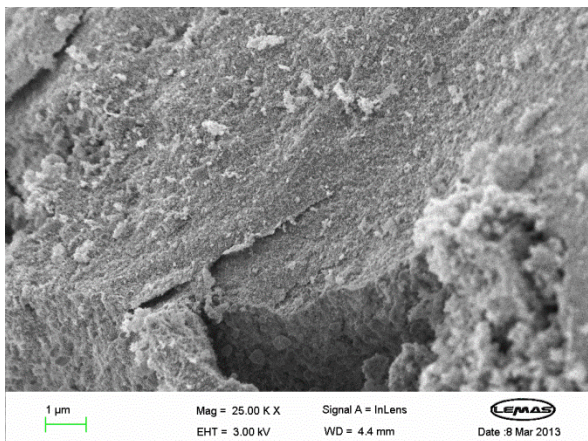
Ni-Ce-Al   Ni-Mn-Al
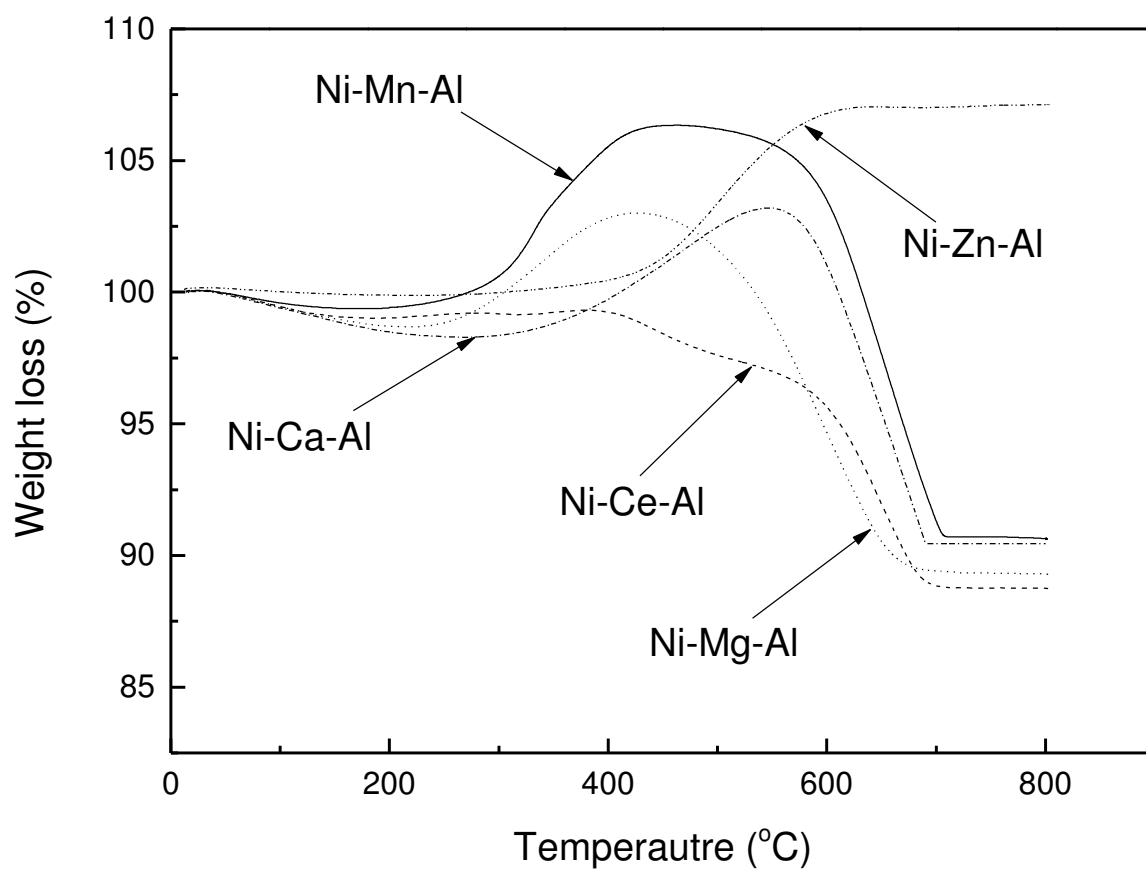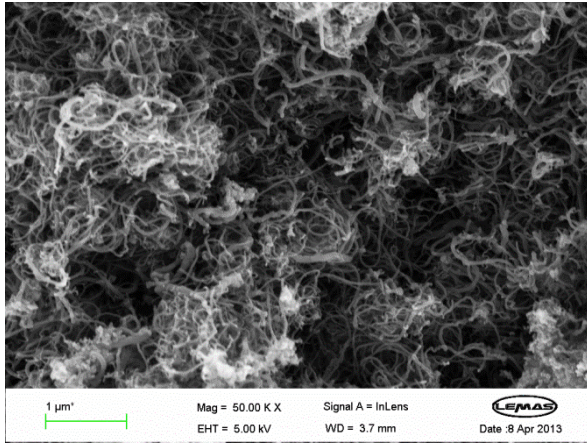
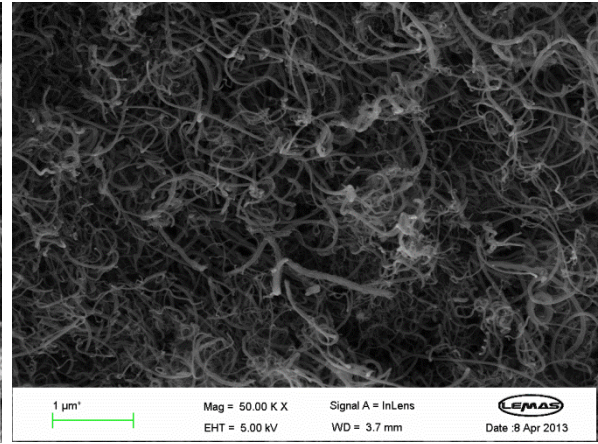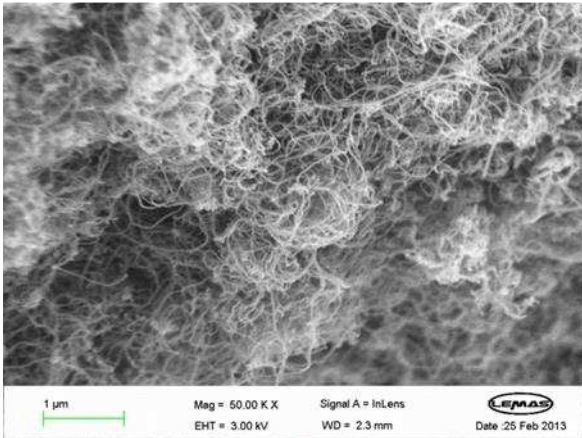**Fig. 3.** Scanning electron micrographs of different reacted catalysts.

Fig. 4. Temperature program oxidation (TPO) analysis of different reacted catalysts in the presence of steam injection.

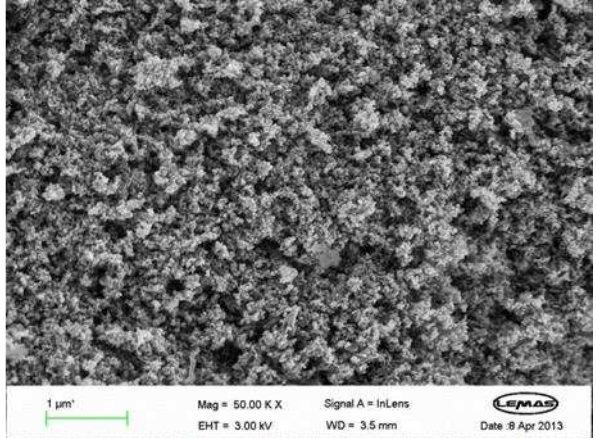Ni-Mn-Al + No steam   Ni-Mn-Al + 2.85 g h^{-1}

Ni-Mn-Al + 4.74 g h^{-1} Ni-Mn-Al + 8.54 g h^{-1}

Fig. 5. Scanning electron micrographs of the reacted Ni-Mn-Al catalyst in the presence of different steam injections.
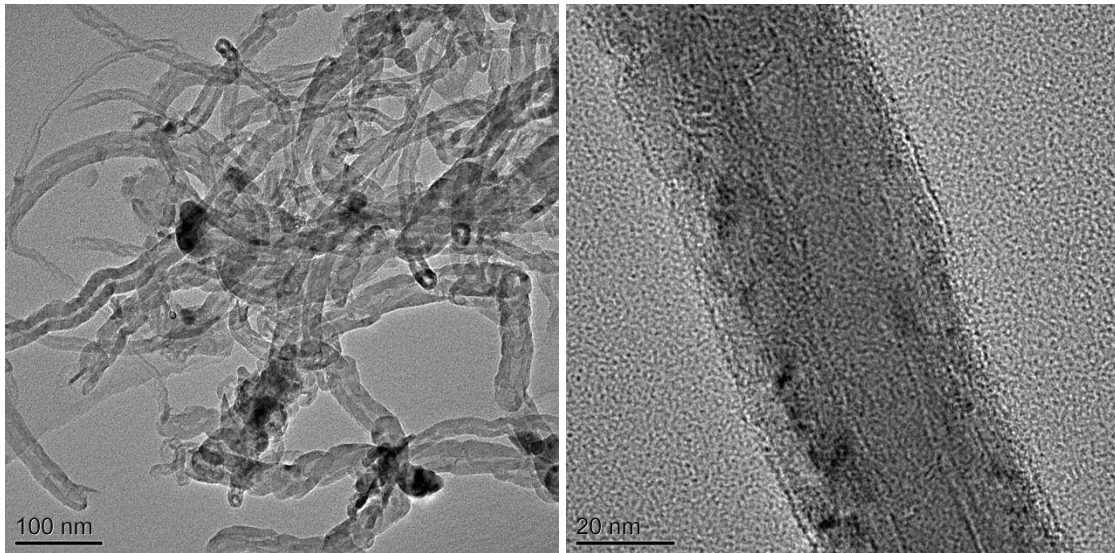
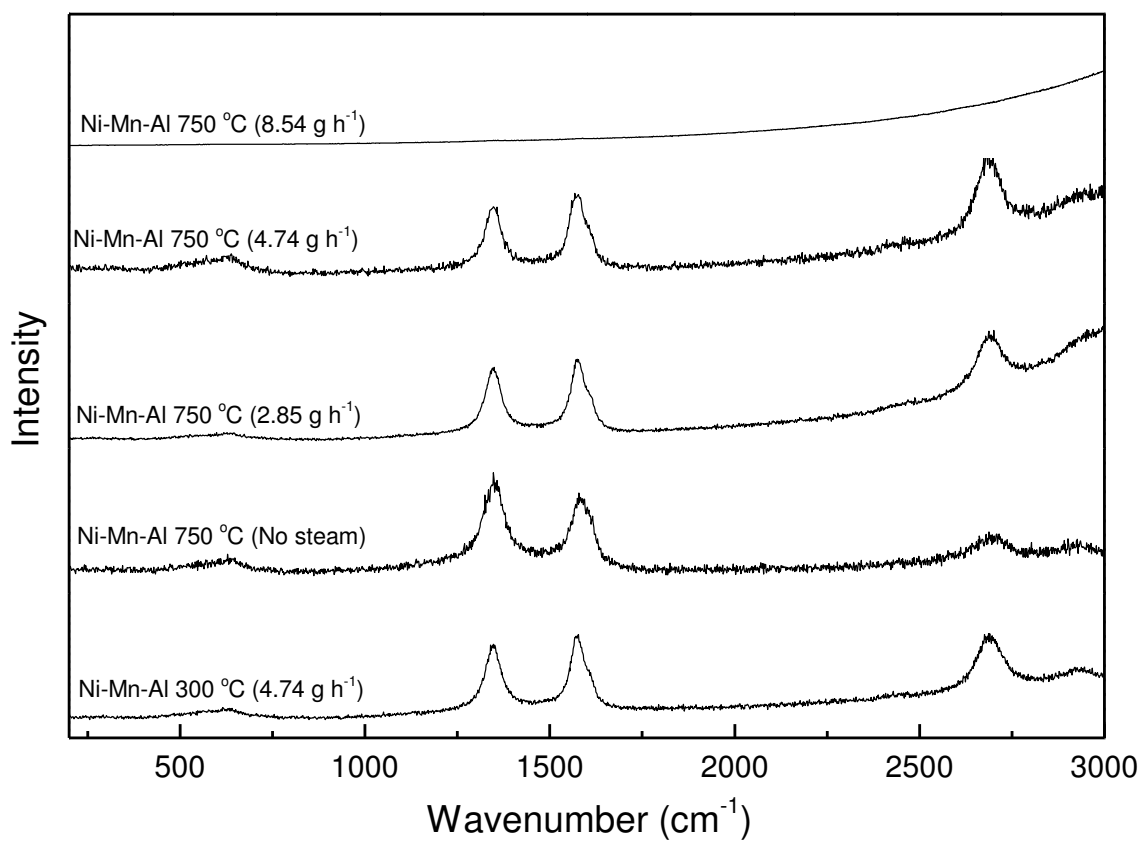**Fig. 6.** TEM analysis of the reacted Ni-Mn-Al catalyst with steam injection of 4.74 g h^{-1}

Fig. 7. Raman spectroscopy of the reacted Ni-Mn-Al catalyst; Ni-Mn-Al reacted at different steam injection rates calcined at 750 °C and Ni-Mn-Al catalyst calcined at 300 °C